

# Graphene-like nanocarbides and nanonitrides of *d* metals (MXenes): synthesis, properties and simulation

Igor R. Shein, Alexander L. Ivanovskii

Institute of Solid State Chemistry, Ural Branch of the Russian Academy of Sciences, 620990 Ekaterinburg, Russia  
E-mail: ivanovskii@ihim.uran.ru

Published in Micro & Nano Letters; Received on 18th October 2012; Accepted on 29th January 2013

Very recently (2011, *Advanced Materials*, 23, 4248), an elegant exfoliation approach was proposed to prepare a new family of two-dimensional (2D)-like transition metal carbides and nitrides from layered MAX phases. This discovery has provided the next stage in the design of new graphene-like inorganic materials with intriguing functionalities and applications. This overview is intended as an introduction to this newest family of graphene-like quasi-2D nanocarbides and nanonitrides of *d* metals, which are known today also as MXenes. Here the authors discuss the available results achieved for MXenes (2011–2012), when a group of various MXenes (2D-Ta<sub>4</sub>C<sub>3</sub>, Ti<sub>3</sub>(C<sub>0.5</sub>N<sub>0.5</sub>)<sub>2</sub>, TiNbC and some others) have been successfully synthesised, a set of their properties (conductivity, mechanical behaviour etc.) were measured and systematical theoretical studies of structural, electronic properties, chemical bonding and the stability of MXenes were initiated. Besides, possible applications of MXenes as promising materials for Li ion batteries, sensors or 2D electronics etc. are noted.

**1. Introduction:** Graphene, the first true one-atom-thick quasi-two-dimensional (2D) crystal, owing to its outstanding properties such as a Dirac spectrum of low-energy quasi-particles, a high electron mobility, an anomalous Hall effect etc., became in the recent years one of the most attractive materials, which is considered as a key element of many future technologies, reviews [1–5].

However, ‘graphene is not the end of the road’ [6]; and a set of new graphene-like materials (free-standing carbon-free 2D crystals) such as single-atom-thick BN (so-called ‘white graphene’) or more complex single-layer-thick MoS<sub>2</sub> or WS<sub>2</sub> were successfully prepared from the corresponding layered three-dimensional (3D) crystals; see [7, 8]. These 3D phases exhibit a sharply anisotropic bonding including strong bonds inside each atomic sheet (or inside molecular layer) against very weak van der Waals-type bonds between the adjacent sheets (layers).

On the other hand, some obvious issues arise in the preparation of graphene-like forms of materials with an isotropic 3D-like system of directional bonds. Such materials include a broad family of transition metal (M) carbides and nitrides with a cubic B1-type structure: MC and MN. These metallic-like phases with outstanding physical properties (enhanced hardness, high melting points, chemical stability, high corrosion resistance etc.) are widely used in the industry as cutting tools, as materials for hard coatings, in high-power energy industry, for optoelectronics etc. [9–11]. Although a set of nanosized carbides and nitrides (such as nanocrystallites [12], hollow polyhedrons [13], monolithic nanorods [14, 15], so-called metallocarbohedrenes [16] etc.) have been synthesised and some other nanoforms (for example, nanotubes or fullerene-like cages [17–19]) have been predicted theoretically, no data on graphene-like forms of transition metal carbides and nitrides were available until recently.

In 2011, a fascinating idea [20] was proposed – to prepare free-standing graphene-like carbides (and nitrides) not from their 3D parent binary phases, but from ternary layered MAX phases (known also as nanolaminates, reviews [21–25]), which include various 2D-like layers of transition metal carbides (or nitrides) as building blocks. These 2D materials are now known as ‘MXenes’; this term denotes their genesis from MAX phases (with the loss of the A component) and their similarity to graphene [20, 26].

The aim of this overview is to emphasise the experimental and theoretical results that may give an insight into the current status

and possible perspectives of MXenes as the newest family of graphene-like materials.

**2. Synthesis and properties:** MAX phases are proposed as precursors for the discussed graphene-like carbides and nitrides (MXenes) [20, 26]. These MAX phases (with the general formula  $M_{n+1}AX_n$ , where  $n = 1, 2$  or  $3$ ;  $M$  are transition *d* metals from groups III–VI;  $X$  are C or N; and  $A$  are Cd, Al, Ga, In, Tl, Si, Ge, Sn, Pb, P, As or S [21–25]) can be described as intergrowth structures consisting of hexagonal blocks  $[M_{n+1}X_n]$  and planar A atomic sheets with a characteristic ‘zigzag’ stacking along the *z*-axis in the sequence  $\dots[M_{n+1}X_n]A[M_{n+1}X_n]A\dots$ , Fig. 1. In turn, carbide (nitride) blocks  $[M_{n+1}X_n]$  have a B1-type structure similar to that of MX binary carbides (nitrides), wherein  $X = C, N$  atoms are located in an octahedral M-atom coordination  $\{M_6X\}$ . As a result, the system of inter-atomic interactions in MAX phases is very anisotropic with strong directional M–X bonds inside blocks  $[M_{n+1}X_n]$ , whereas the bonds between A atoms and between A atomic sheets and blocks  $[M_{n+1}X_n]$  are relatively weak and these A atoms are most reactive [21–25].

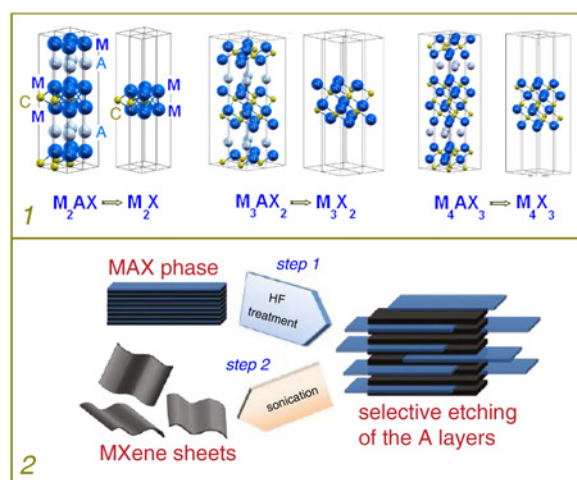


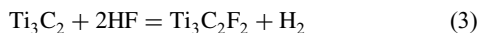
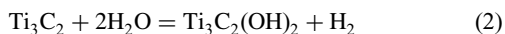
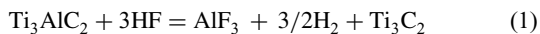
**Figure 1** 1 – Atomic model of preparation of MXenes ( $M_{n+1}X_n$ ) from MAX phases ( $M_{n+1}AX_n$ ) via removing of A sheets [27]  
2 – Schema of realised synthesis [21, 26] of MXenes from MAX phases

**Table 1** Exfoliated Al-containing MAX phases as obtained in [26]

MAX phase	HF conc., %	Time, h	Lattice constant <i>c</i> , nm	
			before HF treatment	after HF treatment
Ti <sub>2</sub> AlC	10	10	1.360	1.504
Ta <sub>4</sub> AlC <sub>3</sub>	50	72	2.408	3.034
(Ti <sub>0.5</sub> , Nb <sub>0.5</sub> ) <sub>2</sub> AlC	50	28	1.379	1.488
(V <sub>0.5</sub> , Cr <sub>0.5</sub> ) <sub>3</sub> AlC <sub>2</sub>	50	69	1.773	2.426
Ti <sub>3</sub> AlCN	30	18	1.841	2.228
Ti <sub>3</sub> AlC <sub>2</sub>	50	2	1.842	2.051

The basic idea [20, 26] was to remove the most weakly bonded sheets of A atoms from the MAX phases and to obtain free-standing blocks [ $M_{n+1}X_n$ ] as novel 2D-like materials, as schematically depicted in Fig. 1.

In the pioneering experiments [20], Ti<sub>3</sub>AlC<sub>2</sub> was taken as an example to extract the most weakly bonded Al sheets from this MAX phase. For this purpose, at the first step, Ti<sub>3</sub>AlC<sub>2</sub> powder was immersed in a Hartree-Fock (HF) solution, when the following reactions occur [20]



In reaction (1) Al atoms were removed and the required samples with the nominal composition Ti<sub>3</sub>C<sub>2</sub> were obtained. The accompanying reactions (2), (3) reflect the formation of hydroxylated or fluorinated Ti<sub>3</sub>C<sub>2</sub> derivatives as a result of the replacement of Al atoms (by fluorine or OH groups) after the reaction with HF, which is conducted in an aqueous environment rich in F ions and OH groups. At the second step, ultrasonication in methanol was used leading to exfoliation of MXenes Ti<sub>3</sub>C<sub>2</sub>. The schema of this two-step process (selective etching → exfoliation) is presented in Fig. 1.

This strategy was further applied to extract the Al sheets from other Al-containing MAX phases [26] such as Ti<sub>2</sub>AlC, Ta<sub>4</sub>AlC<sub>3</sub>, (Ti<sub>0.5</sub>, Nb<sub>0.5</sub>)<sub>2</sub>AlC, (V<sub>0.5</sub>, Cr<sub>0.5</sub>)<sub>3</sub>AlC<sub>2</sub> and Ti<sub>3</sub>AlCN; see Table 1.

The scanning electron microscope (SEM) images (Fig. 2) demonstrate successful exfoliation of MAX phases after the HF treatment and the corresponding X-ray diffraction (XRD) results (Fig. 3) clearly show a drastic loss of crystallinity and structural order for the MAX phases after exfoliation. At the same time, HRTEM and selected area electron diffraction confirm [26] that the crystallinity of the basal MX blocks of the MAX phases is preserved for MXenes.

Today, some properties of MXenes are examined experimentally [20, 26, 29, 30]. So, the exfoliated flakes of MXenes are optically

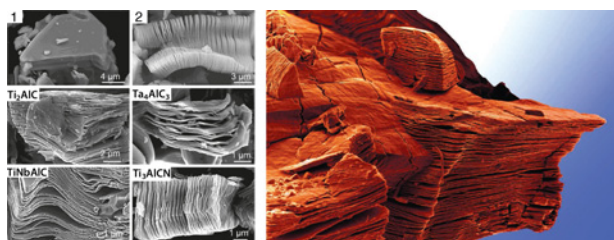


**Figure 2** Secondary electron SEM micrographs for Ti<sub>3</sub>AlC<sub>2</sub> before (1) and after HF treatment (2) and Ti<sub>2</sub>AlC, Ta<sub>4</sub>AlC<sub>3</sub>, TiNbAlC ((Ti<sub>0.5</sub>, Nb<sub>0.5</sub>)<sub>2</sub>AlC) and Ti<sub>3</sub>AlCN after HF treatment producing MXenes [26]. On the right: an electron microscope micrograph for exfoliated Ti<sub>3</sub>AlC<sub>2</sub> [28]

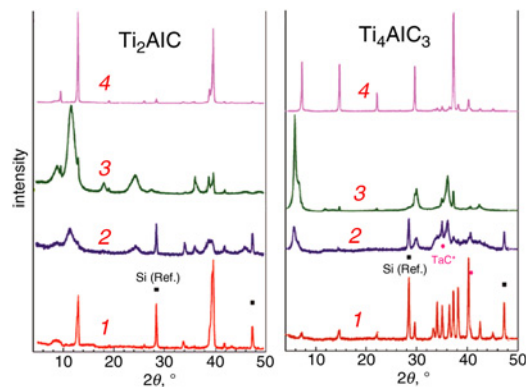


**Figure 3** XRD patterns for Ti<sub>2</sub>AlC and Ta<sub>4</sub>AlC<sub>3</sub>

(1) before HF treatment, (2) after HF treatment, (3) cold-pressed MXene after HF treatment of MAX phases and (4) MAX phase cold-pressed prior to HF treatment [26]. For Ta<sub>4</sub>AlC<sub>3</sub>, a small amount of mono-carbide TaC (with a B1 structure) was present in the initial powder

transparent under visible light. The densities of cold-pressed discs of different MXenes vary between 2.91 g/cm<sup>3</sup> for Ti<sub>2</sub>C and 6.82 g/cm<sup>3</sup> for Ta<sub>4</sub>C<sub>3</sub>. Contact angle measurements with water on pressed MXenes showed a hydrophilic behaviour. The resistivity of the MXenes is higher than for the parent MAX phases – presumably owing to the replacement of Al sheets by OH and/or F [26].

Further development of knowledge of the properties of MXenes is related to the search of possible applications of these materials. For example, electrochemical lithiation and delithiation of MXene Ti<sub>2</sub>C were studied to design a non-aqueous asymmetric cell with a Ti<sub>2</sub>C-based 2D negative electrode [29]. This cell was cycled between 1.0 and 3.5 V and showed a good capacity retention during 1000 galvanostatic charge/discharge cycles. In addition, Li insertion into Ti<sub>2</sub>C was examined for a search of a promising transition metal carbide anode for lithium-ion batteries [30]. The exfoliated Ti<sub>2</sub>C showed reversible capacity about five times higher than the parent phase Ti<sub>2</sub>AlC – mainly because of its open structure, weaker inter-laminar forces and larger specific surface area.

Based on the aforementioned results the possible applications of MXenes as promising materials for Li ion batteries, sensors or as materials for 2D electronics were proposed.

**3. Simulation:** Many of the unique properties of graphene are related to its electronic structure, reviews [1–8]. Therefore it is not surprising that the discovery of the new graphene-like materials (MXenes) has aroused much attention to their electronic properties, which are studied now within ab initio computational approaches. Besides, theoretical simulations of structural, mechanical, magnetic properties, chemical bonding and relative stability of a set of MXenes (the majority of them are Ti-containing systems) are undertaken [20, 27, 31–34].

The optimised atomic structures of the examined MXenes [27, 31–34] reveal that after relaxation, MXenes in general retain the atomic geometries of the corresponding blocks in the parent MAX phases. The inter-atomic distances: *M–M* and *M–X* for MXenes become smaller than for the corresponding MAX phases; the simplest explanation of this is the decrement of the coordination number of *M* atoms in the outer sheets of 2D MXenes. The details of the distortion effects for MXenes (*M*=Ti and *X*=C, N) were also analysed using the calculated [27, 31] distortion indexes  $\alpha_d$ , which are analogues of Hug's indexes [35] for bulk MAX phases and reflect the distortions of {*M*<sub>6</sub>*X*} octahedrons in the examined materials.

Naguib *et al.* [20] used density functional theory (DFT) to reveal the band structure of MXene Ti<sub>3</sub>C<sub>2</sub> as a free-standing 2D structure, as well as of Ti<sub>3</sub>C<sub>2</sub> terminated with fluorine atoms (Ti<sub>3</sub>C<sub>2</sub>F<sub>2</sub>) or OH groups (Ti<sub>3</sub>C<sub>2</sub>(OH)<sub>2</sub>). It was found that unlike the metallic-like

**Table 2** Calculated formation energies ( $E_{\text{form}}$ , eV) for MAX phases  $\text{Ti}_{n+1}\text{AlX}_n$  and MXenes  $\text{Ti}_{n+1}\text{X}_n$  ( $X = \text{C}$  and  $\text{N}$ ,  $n = 1, 2$  and  $3$ ) in some formal reactions as obtained within VASP in [27]

System, equations	$E_{\text{form}}$	System, equations	$E_{\text{form}}$
$\text{Ti}_2\text{AlC} \leftrightarrow \text{TiC} + \text{Al} + \text{Ti}$	-1.17	$\text{Ti}_2\text{C} \leftrightarrow \text{TiC} + \text{Ti}$	1.61
$\leftrightarrow \text{TiC} + \text{TiAl}$	-0.36	$\text{Ti}_2\text{C} \leftrightarrow \text{Ti}_2\text{AlC} - \text{Al}$	2.78
$\text{Ti}_3\text{AlC}_2 \leftrightarrow 2\text{TiC} + \text{Al} + \text{Ti}$	-1.32	$\text{Ti}_3\text{C}_2 \leftrightarrow 2\text{TiC} + \text{Ti}$	1.38
$\leftrightarrow 2\text{TiC} + \text{TiAl}$	-0.51	$\text{Ti}_3\text{C}_2 \leftrightarrow \text{Ti}_3\text{AlC}_2 - \text{Al}$	2.70
$\leftrightarrow \text{Ti}_2\text{AlC} + \text{TiC}$	-0.15		
$\text{Ti}_4\text{AlC}_3 \leftrightarrow 3\text{TiC} + \text{Al} + \text{Ti}$	-1.32	$\text{Ti}_4\text{C}_3 \leftrightarrow 3\text{TiC} + \text{Ti}$	1.43
$\leftrightarrow 3\text{TiC} + \text{TiAl}$	-0.51	$\text{Ti}_4\text{C}_3 \leftrightarrow \text{Ti}_4\text{AlC}_3 - \text{Al}$	2.75
$\leftrightarrow \text{Ti}_2\text{AlC} + 2\text{TiC}$	-0.15		
$\leftrightarrow \text{Ti}_3\text{AlC}_2 + \text{TiC}$	0.00		
$\text{Ti}_2\text{AlN} \leftrightarrow \text{TiN} + \text{Al} + \text{Ti}$	-1.26	$\text{Ti}_2\text{N} \leftrightarrow \text{TiN} + \text{Ti}$	1.74
$\leftrightarrow \text{TiN} + \text{TiAl}$	-0.45	$\text{Ti}_2\text{N} \leftrightarrow \text{Ti}_2\text{AlN} - \text{Al}$	3.00
$\text{Ti}_3\text{AlN}_2 \leftrightarrow 2\text{TiN} + \text{Al} + \text{Ti}$	-1.28	$\text{Ti}_3\text{N}_2 \leftrightarrow 2\text{TiN} + \text{Ti}$	1.79
$\leftrightarrow 2\text{TiN} + \text{TiAl}$	-0.47	$\text{Ti}_3\text{N}_2 \leftrightarrow \text{Ti}_3\text{AlN}_2 - \text{Al}$	3.06
$\leftrightarrow \text{Ti}_2\text{AlN} + \text{TiN}$	-0.02		
$\text{Ti}_4\text{AlN}_3 \leftrightarrow 3\text{TiN} + \text{Al} + \text{Ti}$	-1.46	$\text{Ti}_4\text{N}_3 \leftrightarrow 3\text{TiN} + \text{Ti}$	1.61
$\leftrightarrow 3\text{TiN} + \text{TiAl}$	-0.65	$\text{Ti}_4\text{N}_3 \leftrightarrow \text{Ti}_4\text{AlN}_3 - \text{Al}$	3.06
$\leftrightarrow \text{Ti}_2\text{AlN} + 2\text{TiN}$	-0.20		
$\leftrightarrow \text{Ti}_3\text{AlN}_2 + \text{TiN}$	-0.18		

behaviour of the ‘pure’ MXene  $\text{Ti}_3\text{C}_2$ , its derivatives become narrow-band-gap semiconductors with gaps at about 0.05 and 0.1 eV for  $\text{Ti}_3\text{C}_2(\text{OH})_2$  and  $\text{Ti}_3\text{C}_2\text{F}_2$ , respectively, see also [33]. For  $\text{Ti}_3\text{C}_2(\text{OH})_2$ , its elastic modulus (along the basal plane) was estimated at about 300 GPa [20].

The band structure calculations of the representative group of MXenes  $\text{Ti}_{n+1}\text{C}_n$  and  $\text{Ti}_{n+1}\text{N}_n$  ( $n = 1, 2$  and  $3$ ) [27, 31] reveal that their stability increases with the index  $n$  (or in other words, with the growth of the number of Ti-C(N) bonds), Table 2. For MXenes  $\text{Ti}_{n+1}\text{C}_n$  and  $\text{Ti}_{n+1}\text{N}_n$ , a considerable growth of the density of near-Fermi states  $N(E_F)$  is found and these values become 2.5–4.5 times higher than for the parent MAX phases  $\text{Ti}_{n+1}\text{AlC}_n$  and  $\text{Ti}_{n+1}\text{AlN}_n$  [31]. This effect is explained by redistribution of Ti 3d states from broken Ti-Al bonds to delocalised Ti–Ti metallic-like states placed in the window around the Fermi level, Fig. 4.

The location of the Fermi level  $E_F$  at an intensive density of states (DOS) peak (i.e. a high  $N(E_F)$ ) is indicative of possible magnetic instability. For the first time, this issue was probed numerically using MXenes  $\text{Ti}_3\text{C}_2$  and  $\text{Ti}_3\text{N}_2$  as an example [27, 31]. For both MXenes, the ground state was found to be antiferromagnetic, with ferromagnetic ordering of the spin moments on the Ti atoms within each external Ti sheet, whereas the opposite external titanium sheets are coupled antiferromagnetically. The atomic magnetic moments are  $\sim 0.74 \mu_B$  and  $\sim 0.34 \mu_B$  per a Ti atom for  $\text{Ti}_3\text{C}_2$  and  $\text{Ti}_3\text{N}_2$ , respectively. At the same time, the internal Ti sheets remain practically non-magnetic; and very small magnetic moments ( $< 0.05 \mu_B$ ) are induced on carbon (nitrogen) atoms.

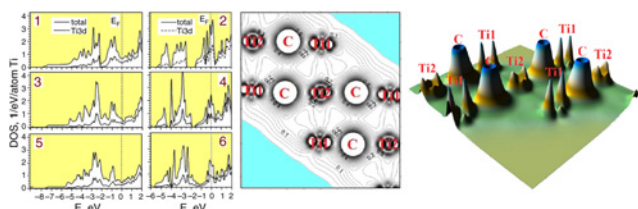


**Figure 4** On the left: Total and Ti 3d densities of states for MXenes  $\text{Ti}_{n+1}\text{C}_n$  and their parent MAX phases  $\text{Ti}_{n+1}\text{AlC}_n$ : 1 –  $\text{Ti}_2\text{AlC}$ ; 2 –  $\text{Ti}_2\text{C}$ ; 3 –  $\text{Ti}_3\text{AlC}_2$ ; 4 –  $\text{Ti}_3\text{C}_2$ ; 5 –  $\text{Ti}_4\text{AlC}_3$ ; 6 –  $\text{Ti}_4\text{C}_3$  [31], which illustrate a considerable growth of the density of near-Fermi states for MXenes – owing to the formation of delocalised Ti–Ti metallic-like states for MXenes, as shown on the example of 2D and 3D electron density maps for  $\text{Ti}_3\text{C}_2$ ; on the right

Further confirmation of long-range magnetic ordering in the external M sheets of MXenes (on the example of  $\text{Ta}_n\text{C}_{n+1}$ ) was received in calculations [32], where local density approximation (LDA), local spin density (LSDA) +  $U$  and Perdew-Burke-Ernzerhof revised for solids (PBEsol) +  $U$  techniques were applied.

Undoubtedly, experimental checking of the predicted magnetic effect seems a non-trivial problem, which requires preparation of atomic-clean free-standing MXenes. On the other hand, covering of MXenes with fluorine ions or OH groups converts these materials into semiconductors [32, 33] and will destroy magnetism. Thus, it may be assumed that via surface chemistry, a rich variety of tunable MXene-based 2D nanomaterials may be produced: semiconductors, non-magnetic or magnetic metals.

In [31] the ‘intermediate’ stage of Al atoms removal from the  $\text{Ti}_{n+1}\text{AlC}_n$  phases, namely the free-standing 2D-like structures with nominal stoichiometry  $\text{Ti}_{n+1}\text{Al}_{0.5}\text{C}_n$ , composed of the two adjacent blocks  $[\text{Ti}_{n+1}\text{C}_n]$  and of Al sheet, that is,  $[\text{Ti}_{n+1}\text{C}_n]/\text{Al}/[\text{Ti}_{n+1}\text{C}_n]$  were simulated.

A potential application of MXenes in Li ion batteries was probed theoretically on the example of 2D  $\text{Ti}_3\text{C}_2$  [33], where a strong Coulomb interaction of adsorbed Li with  $\text{Ti}_3\text{C}_2$  was predicted together with a quite low barrier for Li diffusion and with a high storage capacity of Li – up to  $\text{Ti}_3\text{C}_2\text{Li}_2$ . At the same time, the termination of 2D  $\text{Ti}_3\text{C}_2$  by fluorine ions or by OH groups leads to degradation of these characteristics.

Like graphene, 2D MXenes may be considered as initial systems in the evolution of low-dimensional forms of these materials: 1D (nanotubes, NTs and nanowires, NWs) or 0D (cage-like molecules). This hint was made by the authors [20], who assumed that sonication used for exfoliation can lead to rolling-up of some sheets into scrolls, Fig. 5. The first numerical simulations (within the DFTB approach) of the atomic structure, comparative stability and electronic properties of  $\text{Ti}_2\text{C}$  and  $\text{Ti}_3\text{C}_2$  nanotubes and their hydroxylated forms ( $\text{Ti}_2\text{C}(\text{OH})_2$  and  $\text{Ti}_3\text{C}_2(\text{OH})_2$ ) [34] reveal that the stability of the NTs will increase with the growth of their radii; besides, the tubes with thinner walls ( $\text{Ti}_2\text{C}$ ,  $\text{Ti}_2\text{C}(\text{OH})_2$ ) will be more stable than  $\text{Ti}_3\text{C}_2$  or  $\text{Ti}_3\text{C}_2(\text{OH})_2$  tubes. Another factor of the tubes’ stability is the type of their termination by OH groups. It is of interest that all of the studied nanotubes [34] will be metallic-like – in contrast to their 2D ‘precursors’, whose metallic-like or semiconducting behaviour depends on their atomic configuration. On the other hand, the near-Fermi densities of states (formed mainly by Ti 3d orbitals) for the thinnest  $\text{Ti}_2\text{C}(\text{OH})_2$  tubes change in a wide range, whereas for  $\text{Ti}_3\text{C}_2(\text{OH})_2$  tubes they remain almost independent of the type of OH covering.

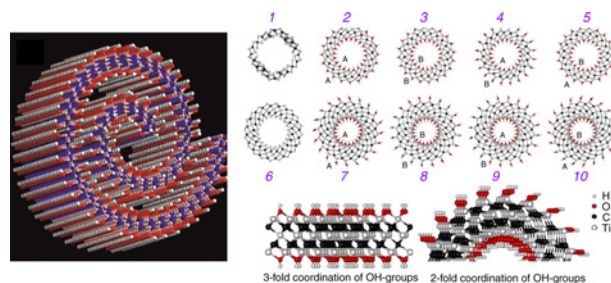


**Figure 5** Schematic view of the atomic structure of the OH-terminated MXene scroll [20] and optimised atomic structures [34] of  $\text{Ti}_2\text{C}$  (1),  $\text{Ti}_3\text{C}_2$  (2),  $\text{Ti}_2\text{C}(\text{OH})_2$  (2–5) and  $\text{Ti}_3\text{C}_2(\text{OH})_2$  (7–10) based armchair (10,10) nanotubes: the top views are shown

Indexes A and B denote various types of OH termination of inner and outer walls of the tubes. For asymmetric configurations  $A/\text{TiC}_x/B$ , two possible types of nanotubes are probed:  $A@/\text{TiC}_x@/B$  and  $B@/\text{TiC}_x@/A$  (4,5 and 9,10). For  $\text{Ti}_3\text{C}_2(\text{OH})_2$  NTs, the external OH-groups adopt a two-fold coordination owing to a considerable surface curvature – as depicted on the bottom panel

**4. Conclusions and outlook:** The main goal of this overview is to highlight the main experimental and theoretical results that may give an insight into the current status and possible perspectives of the newest family of graphene-like nanocarbitides and nanonitrides of *d* metals: so-called MXenes.

The achieved advancements in synthetic strategy and basic research together with some interesting possible applications of MXenes give a strong impetus to the further progress in physics and chemistry of these 2D nanomaterials.

At the same time, a lot of challenges for the immediate future remain. In our opinion, the most urgent issue is the development of principles of functionalisation and the corresponding preparation techniques, which will allow MXenes to be produced with controllable properties – for example, through the introduction of structural vacancies and/or impurities, by adsorption of atoms or molecules, by formation of various derivatives (oxides, hydrides etc.) or more complex MXene-based composites. Besides, the search for new, unknown till now 0D and 1D forms of MXenes such as nanocones, nanoribbons etc., seems very desirable. Here, the combination of experimental efforts with the development of theoretical models will be useful.

## 5 References

- Castro Neto A.H., Guinea F., Peres N.M.R., Novoselov K.S., Geim A.K.: ‘The electronic properties of graphene’, *Rev. Mod. Phys.*, 2009, **81**, p. 109. <http://dx.doi.org/10.1103/RevModPhys.81.109>
- Rozhkov A.V., Giavaras G., Bliokh Y.P., Freilikher V., Nori F.: ‘Electronic properties of mesoscopic graphene structures: charge confinement and control of spin and charge transport’, *Phys. Rep.*, 2011, **503**, p. 77. Accepted 1 February 2011. Available online 22 February 2011. Editor: D.L. Mills. <http://dx.doi.org/10.1016/j.physrep.2011.02.002>
- Singh V., Joung D., Zhai L., Das S., Khondaker S.I., Seal S.: ‘Graphene based materials: past, present and future’, *Prog. Mater. Sci.*, 2011, **56**, p. 1178. <http://dx.doi.org/10.1016/j.pmatsci.2011.03.003>
- Huang X., Yin Z., Wu S., Qi X., He Q., Zhang Q., Yan Q., Boey F., Zhang H.: ‘Graphene-based materials: synthesis, characterization, properties, and applications’, *Small*, 2011, **7**(14), p. 7. <http://dx.doi.org/10.1002/sml.201002009>
- Yan L., Zheng Y.B., Zhao F., Li S., Gao X., Xu B., Weiss P.S., Zhao Y.: ‘ChemInform abstract: chemistry and physics of a single atomic layer: strategies and challenges for functionalization of graphene and graphene-based materials’, *Chem. Soc. Rev.*, 2012, **41**, p. 97. <http://dx.doi.org/10.1002/chem.201213274>
- Castro Neto A.H., Novoselov K.S.: ‘New directions in science and technology: two-dimensional crystals’, *Rep. Prog. Phys.*, 2011, **74**, p. 082501. <http://dx.doi.org/10.1088/0034-4885/74/8/082501>
- Rao C.N.R., Nag A.: ‘Inorganic analogues of graphene’, *Eur. J. Inorg. Chem.*, 2010, **27**, p. 4244. <http://dx.doi.org/10.1002/ejic.201000408>
- Ivanovskii A.L.: ‘Graphene-based and graphene-like materials’, *Russ. Chem. Rev.*, 2012, **81**, p. 571. <http://dx.doi.org/10.1070/RC2012v081n07ABEH004302>
- Toth L.E.: ‘Transition metal carbides and nitrides’ (Academic, New York, 1971)
- Oyama T.: ‘The chemistry of transition metal carbides and nitrides’ (Springer, New York, 1996)
- Lengauer W.: ‘Transition metal carbides, nitrides and carbonitrides’ (Wiley-VCH, Weinheim, 2000)
- Lu Q., Hu J., Tang K., Deng B., Qian Y., Zhou G., Liu X.M.G.: ‘The co-reduction route to TiC nanocrystallites at low temperature’, *Chem. Phys. Lett.*, 1999, **314**, p. 37. [http://dx.doi.org/10.1016/S0009-2614\(99\)01109-4](http://dx.doi.org/10.1016/S0009-2614(99)01109-4)
- Bai Y.J., Feng X., Lü B., Wang C.G., Qi Y.X., Liu Y.X., Zhu B., Wang Y.X.: ‘Novel synthesis of nanocrystalline TiC hollow polyhedrons’, *Chem. Phys. Lett.*, 2004, **388**, p. 58. <http://dx.doi.org/10.1016/j.cplett.2004.02.074>
- Wong E.W., Maynor B.W., Burns L.D., Lieber C.M.: ‘Growth of metal carbide nanotubes and nanorods’, *Chem. Mater.*, 1996, **8**, p. 2041. <http://dx.doi.org/10.1021/cm960083b>
- Liang C.H., Meng G.W., Chen W., Wang Y.W., Zhang L.D.: ‘Growth and characterization of TiC nanorods activated by nickel nanoparticles’, *J. Cryst. Growth*, 2000, **220**, p. 296. [http://dx.doi.org/10.1016/S0022-0248\(00\)00849-6](http://dx.doi.org/10.1016/S0022-0248(00)00849-6)
- Rohmer M.M., Benard M., Poble J.M.: ‘Structure, reactivity, and growth pathways of metallocarbohedrenes  $M_8C_{12}$  and transition metal/carbon clusters and nanocrystals: a challenge to computational chemistry’, *Chem. Rev.*, 2000, **100**, p. 495. <http://dx.doi.org/10.1021/cr9803885>
- Enyashin A.N., Ivanovskii A.L.: ‘Structural and electronic properties of the TiC nanotubes: density functional-based tight binding calculations’, *Physica E* **30**, 2005, pp. 164–168. <http://dx.doi.org/10.1016/j.physe.2005.08.004>
- Li S.F., Xue X., Jia Y., Zhao G., Zhang M., Gong X.G.: ‘Stable cubic metal-semiconductor alloy clusters:  $X_4Z_4$  ( $X=Cu, Ag, Au, Ti$ ;  $Y=C, Si$ )’, *Phys. Rev.*, 2006, **73**, p. 165401. <http://dx.doi.org/10.1103/PhysRevB.73.165401>
- Enyashin A.N., Ivanovskii A.L.: ‘Structural, cohesive and electronic properties of titanium oxycarbides ( $TiC_xO_{1-x}$ ) nanowires and nanotubes: DFT modeling’, *Chem. Phys.*, 2009, **362**, p. 58. <http://dx.doi.org/10.1016/j.chemphys.2009.06.004>
- Naguib M., Kurtoglu M., Presser V., Lu J., Niu J., Heon M., Hultman L., Gogotsi Y., Barsoum M.W.: ‘Two-dimensional nanocrystals produced by exfoliation of  $Ti_3AlC_2$ ’, *Adv. Mater.*, 2011, **23**, p. 4248. <http://dx.doi.org/10.1002/adma.201102306>
- Barsoum M.W.: *Prog. Solid State Chem.*, 2000, **28**, p. 201
- Wang J., Zhou Y.: ‘Recent progress in theoretical prediction, preparation, and characterization of layered ternary transition-metal carbides’, *Annu. Rev. Mater. Res.*, 2009, **39**, p. 415. <http://dx.doi.org/10.1146/annurev-matsci-082908-145340>
- Eklund P., Beckers M., Jansson U., Högberg H., Hultman L.: ‘The  $M_{n+1}AX_n$  phases: materials science and thin-film processing’, *Thin Solid Films*, 2010, **518**, p. 1851. <http://dx.doi.org/10.1016/j.tsf.2009.07.184>
- Medvedeva N.I., Enyashin A.N., Ivanovskii A.L.: ‘Modeling of the electronic structure, chemical bonding, and properties of ternary silicon carbide  $Ti_3SiC_2$ ’, *J. Struct. Chem.*, 2011, **52**, p. 785. <http://dx.doi.org/10.1134/S0022476611040226>
- Sun Z.M.: ‘Progress in research and development on MAX phases: a family of layered ternary compounds’, *Intern. Mater. Rev.*, 2011, **56**, p. 143. <http://dx.doi.org/10.1179/1743280410Y.0000000001>
- Naguib M., Mashtalir O., Carle J., Presser V., Lu J., Hultman L., Gogotsi Y., Barsoum M.W.: ‘Two-dimensional transition metal carbides’, *ASC Nano*, 2012, **6**, p. 1322. <http://dx.doi.org/10.1021/nl204153h>
- Shein I.R., Ivanovskii A.L.: ‘Graphene-like titanium carbides and nitrides  $Ti_{n+1}C_n$ ,  $Ti_{n+1}N_n$  ( $n=1, 2$ , and 3) from de-intercalated MAX phases: first-principles probing of their structural, electronic properties and relative stability’, *Comput. Mater. Sci.*, 2012, **65**, pp. 104–114. <http://dx.doi.org/10.1016/j.commatsci.2012.07.011>
- Anasori B., Naguib M., Gogotsi Y., Barsoum M.W.: *Science*, 2012, **335**, p. 527
- Come J., Naguib M., Rozier P., Barsoum M.W., Gogotsi Y., Taberna P.-L., Morcrette M., Simon P.: ‘A non-aqueous asymmetric cell with a  $Ti_2C$ -based two-dimensional negative electrode’, *J. Electrochem. Soc.*, 2012, **159**, p. A1368. <http://dx.doi.org/10.1149/2.003208jes>
- Naguib M., Come J., Dyatkin B., Presser V., Taberna P.-L., Simon P., Barsoum M.W., Gogotsi Y.: ‘MXene: a promising transition metal carbide anode for lithium-ion batteries’, *Electrochem. Commun.*, 2012, **16**, p. 61. <http://dx.doi.org/10.1016/j.elecom.2012.01.002>
- Shein I.R., Ivanovskii A.L.: ‘Planar nano-block structures  $Ti_{n+1}AlO_5C_n$  and  $Ti_{n+1}C_n$  ( $n=1$ , and 2) from MAX phases: structural, electronic properties and relative stability from first principles calculations’, *Superlattices Microstruct.*, 2012, **52**, p. 147. <http://dx.doi.org/10.1016/j.spmi.2012.04.014>
- Lane N.J., Barsoum M.W., Rondinelli J.M.: ‘Electronic structure and magnetism in two-dimensional hexagonal 5d transition metal carbides,  $Tan+1Cn$  ( $n=1, 2, 3$ )’, arXiv:1210.1241 (2012)
- Tang Q., Zhou Z., Shen P.: ‘Are MXenes promising anode materials for Li Ion batteries? Computational studies on electronic properties and Li storage capability of  $Ti_3C_2$  and  $Ti_3C_2X_2$  ( $X=F, OH$ ) Monolayer’, *J. Am. Chem. Soc.*, 2012, **134**, p. 16909. <http://dx.doi.org/10.1021/ja308463r>
- Enyashin A.N., Ivanovskii A.L.: ‘Atomic structure, comparative stability and electronic properties of hydroxylated  $Ti_2C$  and  $Ti_3C_2$  nanotubes’, *Comput. Theor. Chem.*, 2012, **989**, p. 27. <http://dx.doi.org/10.1016/j.comptc.2012.02.034>
- Hug G.: ‘Electronic structures of and composition gaps among the ternary carbides  $Ti_2MC$ ’, *Phys. Rev. B*, 2006, **74**, p. 184113. <http://dx.doi.org/10.1103/PhysRevB.74.184113>